Structural and Thermal Stability Characterization of Escherichia coli D-Galactose/D-Glucose-Binding Protein

ARTICLE *in* BIOTECHNOLOGY PROGRESS · SEPTEMBER 2008

Impact Factor: 2.15 · DOI: 10.1021/bp0341848 · Source: PubMed

Structural and Thermal Stability Characterization of *Escherichia coli* D-Galactose/D-Glucose-Binding Protein

Sabato D'Auria,*,†,‡ Fabrizio Alfieri,‡ Maria Staiano,‡ Fabrizio Pelella,‡ Mose' Rossi,‡,§ Andrea Scirè,|| Fabio Tanfani,|| Enrico Bertoli,|| Zigmunt Grycznyski,† and Joseph R. Lakowicz†

University of Maryland at Baltimore, Center for Fluorescence Spectroscopy, 725 W Lombard Street, Baltimore Maryland 21201, Institute of Protein Biochemistry, CNR, Via P. Castellino, 111 80131 Naples, Italy, Department of Biological Chemistry, University of Naples Federico II, Naples, Italy, and Istituto di Biochimica, Università Politecnica delle Marche, Via Ranieri, 60131 Ancona, Italy

The effect of temperature and glucose binding on the structure of the galactose/glucose-binding protein from *Escherichia coli* was investigated by circular dichroism, Fourier transform infrared spectroscopy, and steady-state and time-resolved fluorescence. The data showed that the glucose binding induces a moderate change of the secondary structure content of the protein and increases the protein thermal stability. The infrared spectroscopy data showed that some protein stretches, involved in α-helices and *β* strand conformations, are particularly sensitive to temperature. The fluorescence studies showed that the intrinsic tryptophanyl fluorescence of the protein is well represented by a three-exponential model and that in the presence of glucose the protein adopts a structure less accessible to the solvent. The new insights on the structural properties of the galactose/glucose-binding protein can contribute to a better understanding of the protein functions and represent fundamental information for the development of biotechnological applications of the protein.

Introduction

The periplasm of Gram-negative bacteria contains a large family of specific binding proteins that are essential primary receptors in transport and, in a few cases, chemotaxis (*1*). These proteins usually have a monomeric structure that folds in two main domains linked by three strands commonly referred to as the hinge region. Conformational changes involving the hinge are thought to be necessary for sugars to get in and out of the protein-binding site (*2*). Differences in the structures of the ligand-bound and ligand-free proteins are essential for their proper recognition by the membrane components (*3*). This property of binding proteins makes them good candidates as biological recognition elements in the development of biosensors (*4*). In fact, in the presence of a specific ligand, these proteins undergo a large conformational change in their global structure to accommodate the ligand inside the binding site (*5*). Based on this conformational change, sensing systems for maltose and glucose were developed using their respective binding proteins (*6*, *7*).

D-Galactose/D-glucose-binding protein (GGBP) of *Escherichia coli* serves as an initial component for both chemotaxis toward galactose and glucose and high-affinity active transport of the two sugars. Well-refined structures of GGBP in the absence and in the presence of glucose have provided a view at the molecular level of the sugar-binding site (*8*). Several research labs are studying the biotechnological applications of GGBP as glucose sensor (*9*, *10*), and recently, some of us have demonstrated that proteins that bind glucose can be used as probes to develop a low-cost lifetime-based glucose sensor (*4*, *10*).

Knowledge of details on structural and stability properties of a protein are needed when planning particular biotechnological applications. In this context, we have investigated the effect of glucose on the structure and stability of GGBP from *E. coli*. The secondary structure of the protein in the absence and in the presence of the sugar was studied by means of circular dichroism (CD) and Fourier transform infrared (FT-IR) spectroscopy in the range of 10−95 °C. Frequency-domain measurements were used to investigate the conformational dynamics of GGBP. Our results show that glucose slightly modifies the secondary structure content of GGBP and increases the protein thermal stability.

Materials and Methods

Materials. Deuterium oxide (99.9% ^2H_2O), ^2HCl, and NaO^2H were purchased from Aldrich. Hepes and D-glucose were obtained from Sigma. All other chemicals used were commercial samples of the purest quality.

Preparation and Purification of GGBP. D-Galactose/D-glucose-binding protein from *E. coli* was prepared and purified according to Tolosa et al. (*4*). To remove the endogenous glucose from GGBP, the protein solution was loaded on a Sephadex G-10 column (Amersham). The protein used in all the measurements was considered sugar-free.

* To whom correspondence should be addressed. Phone: +39-0816132250. Fax: +39-0816132277. E-mail: dauria@dafne.ibpe.na.cnr.it.

† University of Maryland at Baltimore.

‡ Institute of Protein Biochemistry, CNR.

§ University of Naples Federico II.

|| Università Politecnica delle Marche.

10.1021/bp0341848 CCC: $27.50
Published on Web 08/27/2003

Protein Assay. The protein concentration was determined by the method of Bradford (*11*) by measuring the absorbance at 595 nm in a double beam Cary 1E spectrophotometer (Varian, Mulgrade, Victoria, Australia). We used bovine serum albumin as standard.

Circular Dichroism Spectroscopy. Circular dichroism (CD) spectroscopy was performed on homogeneous samples of GGBP at concentrations of 0.2 mg/mL in 1.0 mM Hepes/NaOH buffer, pH 7.0, plus the specified amounts of glucose. We used a J-710 spectropolarimeter (Jasco, Tokyo, Japan) equipped with the Neslab RTE-110 temperature-controlled liquid system (Neslab Instruments, Portsmouth, NH) and calibrated with a standard solution of (+)-10-camphorsulfonic acid. Sealed cuvettes with a 0.1 cm path length (Helma, Jamaica, NJ) were used. Photomultiplier voltage did not exceed 600 V in the spectral regions measured. Each spectrum was averaged five times and smoothed with Spectropolarimeter System Software version 1.00 (Jasco, Japan). All measurements were performed under nitrogen flow. Before undergoing CD analyses, all samples were kept at the temperature being studied for 10 min (*12*). The results are expressed in terms of molar ellipticity (θ).

Preparation of Samples for Infrared Measurements. About 1.5 mg of protein, dissolved in the buffer used for its purification, was centrifuged in a 10 K Centricon microconcentrator (Amicon) at 3000 × *g* at 4 °C and concentrated into a volume of approximately 30 μL. Then, 250 μL of 25 mM Hepes/NaOH or 250 μL of 25 mM Hepes/NaOH, 10 mM glucose buffer, pH 7.0 was added, and the sample was concentrated again. The same procedure was used for buffers prepared in ^2H_2O, p^{2}H 7.0. The p^{2}H value corresponds to the pH meter reading + 0.4 (*13*). The washings were repeated several times in order to completely replace the original buffer with the buffer used in a particular experiment. Washings took 24 h, which is the time of contact of the protein with the ^2H_2O or H_2O media prior FT-IR analysis. In the last washing the protein samples were concentrated to a final volume of approximately 35 μL and used for the infrared measurements.

Infrared Spectra. The concentrated protein samples were placed in a thermostated Graseby Specac 20 500 cell (Graseby-Specac Ltd, Orpington, Kent, UK) fitted with CaF_2 windows and a 6 μm tin spacer or a 25 μm Teflon spacer for the experiments in H_2O or ^2H_2O, respectively. FT-IR spectra were recorded by means of a Perkin-Elmer 1760-x Fourier transform infrared spectrometer using a deuterated triglycine sulfate detector and a normal Beer-Norton apodization function. For at least 24 h before and during data acquisition the spectrometer was continuously purged with dry air at a dew point of −40 °C. Spectra of buffers and samples were acquired at 2 cm^{-1} resolution under the same scanning and temperature conditions. In the thermal denaturation experiments, the temperature was raised in 5 °C steps from 20 to 95 °C using an external bath circulator (HAAKE F3). The actual temperature in the cell was controlled by a thermocouple placed directly onto the window. Spectra were collected and processed using the SPECTRUM software from Perkin-Elmer. Correct subtraction of H_2O was judged to yield an approximately flat baseline at 1900−1400 cm^{-1}, and subtraction of ^2H_2O was adjusted to the removal of the ^2H_2O bending absorption close to 1220 cm^{-1} (*14*). The deconvoluted parameters were set with a gamma value of 2.5 and a smoothing length of 60. Second derivative spectra were calculated over a 9-data-point range (9 cm^{-1}).

In the spectra obtained in ^2H_2O medium, the percentage of ^{1}H/^{2}H exchange was obtained by the intensity of the residual amide II band at 1550 cm^{-1} (*15*). In particular, the calculations were performed after normalization of the amide I and amide I′ bands to 1.0 absorbance value. In the spectrum of the protein recorded in H_2O the intensity at 1550 cm^{-1} was considered corresponding to 100% of amide hydrogens (^{1}H). Full ^{1}H/^{2}H exchange was considered to occur at 98 °C, the temperature at which the protein was completely unfolded. In this spectrum the intensity at 1550 cm^{-1} was taken as a reference for 0% of amide hydrogens (^{1}H) (*16*).

The estimation of the secondary structure composition was carried out by curve fitting of the absorbance of the amide I′ band (*17*) and using the software GRAMS (Galactic Industries Corporation, U.S.A.).

Fluorescence Spectroscopy. Emission spectra were obtained with a Varian Cary Eclipse spectrofluorometer, at a protein concentration 0.05 mg/mL in 1.0 mM Hepes/NaOH buffer, pH 7.0, plus the specified amount of glucose. The excitation was set at 295 nm in order to exclude the tyrosine contribution to the overall fluorescence emission. All the fluorescence data were corrected for the dependence of temperature. Frequency domain data were obtained with a frequency domain fluorometer operating between 2 and 2000 MHz (*18*−*20*). The modulated excitation was provided by the harmonic content of a laser pulse train with a repetition rate of 3.75 MHz and a pulse width of 5 ps, from synchronously pumped and cavity dumped rhodamine 6G dye laser. The dye laser was pumped with a mode-locked argon ion laser (Coherent, Innova 100). The dye laser output was frequency doubled to 300 nm for tryptophan excitation. For intensity decay measurements, magic angle polarizer orientations were used. The emitted light was observed through an interference filter at 340 nm.

The frequency-domain intensity data were fit to the time-resolved expression

$$I(t) = \sum_i \alpha_i e^{-t/\tau_i}$$

where α_i are the pre-exponential factors, t is the decay time, and $\Sigma\alpha_i = 1.0$.

The mean lifetime is given by

$$\bar{\tau} = \frac{\sum_i \alpha\tau^2}{\sum_i \alpha\tau}$$

Results

Escherichia coli GGBP is a monomeric protein of molecular weight of about 32 kDa, containing five residues of tryptophan. The sugar-binding site is located in the cleft between the two lobes of the bilobate protein. In Figure 1 is shown a close view of the binding site of *Escherichia coli* GGBP and the amino acids directly involved in glucose binding. Binding specificity and affinity are conferred primarily by polar planar side-chain residues that form an intricate network of cooperative and bidentate hydrogen bonds with the sugar substrate and secondarily by aromatic residues that sandwich the pyranose ring (*8*).

Circular Dichroism Analyses. At 25 °C the CD spectra in the far-ultraviolet region of GGBP and GGBP in the presence of 10 mM glucose (GGBP/Glc) are almost superimposable, indicating that the overall secondary

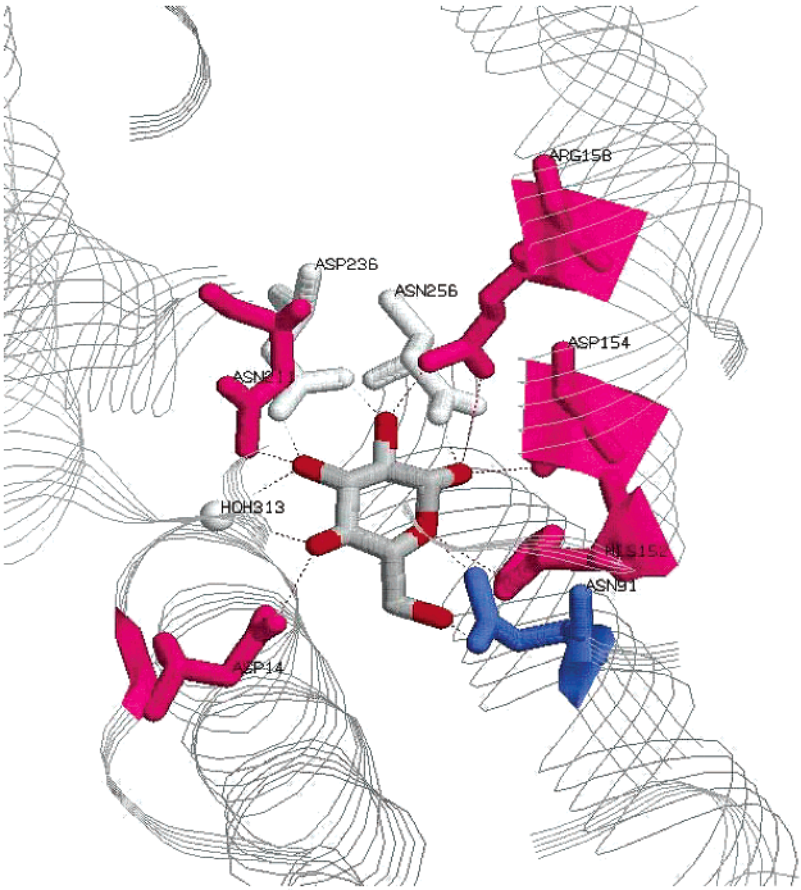

Figure 1. Close view of the binding site of *Escherichia coli* GGBP. The amino acids directly involved in glucose binding are colored by the *RasMol* structure color scheme. Amino acids belonging to α-helices, turns, and unordered structure are colored, respectively, magenta, pale blue, and white. Dotted lines represent the hydrogen bonds. Arg158, Asp154, and His152 belong to the same α-helix where His152 is at its end. Asn211 and Asp14 belong to another two different α-helices, and they are both at the terminal end of their respective helix. The figure was created using *RasMol* Version 2.7 by H. Bernstein and the molecule coordinates from the PDB file 2GBP created 15-Jul-1990 by N. K. Vyas, M. N. Vyas, and F. A. Quiocho.

structural organization of the protein is only slightly affected by the addition of 10 mM glucose (spectra not shown). In fact, the estimation of the secondary structure content of the protein reveals a small increase of the α-helices induced by the addition of glucose (data not reported).

Figure 2 shows the effect of 10 mM glucose on the α-helices content of GGBP in the temperature range of 20−90 °C. Addition of glucose to the protein solution results in a marked increase of the melting temperature (T_m) of GGBP. In fact, in the presence of the sugar the T_m value of GGBP increases from 58 to 64 °C.

Absorbance, Resolution-Enhanced FT-IR Spectra, and Secondary Structure of GGBP. Figure 3 shows the original IR absorbance spectra of GGBP in H_2O and ^2H_2O. In H_2O, the amide I and amide II bands show a maximum at 1653.4 and 1549.4 cm^{-1}, respectively. In ^2H_2O the amide I′ band is located at 1644.7 cm^{-1}, and the amide II is present as a small shoulder (1553.5 cm^{-1}) in the spectrum. The bandshift to lower wavenumber of amide I and the marked decrease in intensity of the amide II band are due to the exchange of amide hydrogens with deuterium ($^1H/^2H$) (*15*). In particular, the decrease of the amide II band intensity gives a measure of the accessibility of the solvent (^2H_2O) to the protein: the higher the intensity decreases, the higher the solvent accessibility (*15*). In the spectrum obtained in heavy water, the residual amide II band indicates that ^2H_2O was not completely accessible to GGBP and, in turn, suggests that part of the protein possesses a particularly

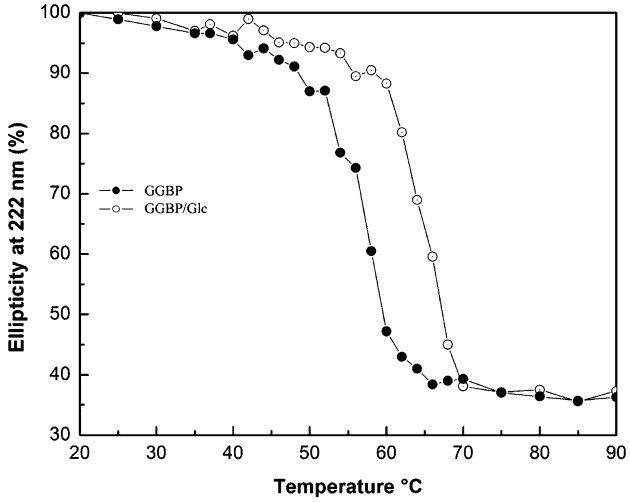

Figure 2. Circular dichroic activity at 222 nm of GGBP and GGBP/Glc in the range of temperature 20−90 °C.

compact structure. We estimated that 42% of amide hydrogens were not exchanged in the protein sample. In the presence of 10 mM glucose, and under the same temperature conditions as the previous sample, the unexchanged hydrogens were 44%. The increase in temperature led to further $^1H/^2H$ exchange that reached 100% when the protein became completely unfolded.

The deconvoluted and second derivative spectra of GGBP in H_2O show amide I component bands at 1680.5,

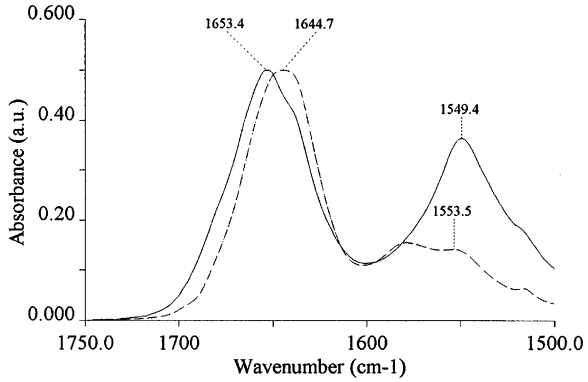

Figure 3. Original absorbance spectra of GGBP at 20 °C, pH or p^{2}H 7.0. Continuous and dashed lines refer to spectra of GGBP in H_2O and ^2H_2O, respectively.

1665.0, 1653.2, and 1637.8 cm^{-1} and the amide II centered at 1550.0 cm^{-1} (spectra not shown). In ^2H_2O medium, the resolution-enhanced spectra of GGBP in the absence and in the presence of 10 mM glucose (Figure 4), reveal two α-helix bands at 1658.2 and 1650.7 cm^{-1} (*21*) that could represent two different populations of helices differing in exposition to the solvent (^2H_2O) or in the regularity of folding (distortion) (*22*). The 1697.3, 1636.6, and 1627.2 cm^{-1} bands are due to *β*-sheets; this multiplicity reflects differences in the hydrogen bonding strength as well as differences in transition dipole coupling in different *β*-strands (*23*). In particular, the 1627.2 cm^{-1} band may be due to *β*-strands particularly exposed to the solvent, i.e., *β*-strands at the edge of a *β*-sheet (termed *β*-edge) that are not hydrogen bonded to another polypeptide extended chain but to a different intra- or intermolecular structure (*21*, *24*, *25*) or to an unusually strongly hydrogen bonded *β*-sheet (*25*, *26*). The 1663 cm^{-1} band reveals turns, whereas the 1674.0 and 1680.9 cm^{-1} peaks may be due to turns and/or *β*-sheet (*21*, *26*). The bands below 1620 cm^{-1} are due to amino acid side-chain absorption, except the 1550.5 cm^{-1} band, which is due to residual amide II band absorption. In particular, the 1582.0 cm^{-1} peak is due to the ionized carboxyl group of aspartic acid and the 1515.2 cm^{-1} one is characteristic of tyrosine residues (*27*).

As shown in Figure 4, the presence of glucose does not affect remarkably the secondary structure of the protein. A small increase in the 1658.2 cm^{-1} band intensity in the second derivative spectrum, which is less evident in the deconvoluted one, suggests that the sugar may have altered slightly the content of α-helices. To check this possibility we estimated the secondary structure composition of the protein in the absence and in the presence of glucose. The results reported in Table 1 show an increase in the area of the band close to 1658 cm^{-1}, supporting the indication of resolution-enhanced spectra and the CD data.

Table 1. Calculated Positions and Fractional Areas (%) of the Amide I′ (1700−1600 cm^{-1}) Component Bands for GGBP and GGBP/Glc[a]

band position (cm^{-1})	assignment	band area (%)	
		GGBP	GGBP/Glc
1694	*β*	1	1
1680	t/*β*	6	6
1673	t/*β*	4	4
1665	t	14	12
1658	α	5	9
1651	α	36	34
1643	u	11	10
1636	*β*	17	17
1628	*β*	6	7

[a] The curve fitting was carried out on the absorbance spectra obtained at 20 °C. The symbols α, *β*, t, and u stand for α-helix, *β*-sheet, turns and unordered structures, respectively.

Thermal Stability of GGBP. The deconvoluted (spectra not shown) and second derivative spectra of the protein in the absence of glucose indicate that the secondary structure elements belonging to the 1658.2 and 1627.2 cm^{-1} bands are particularly sensitive to temperature since the intensity of these bands decreased at relatively low temperatures (Figure 5, bottom set of spectra). In particular, the 1658.2 cm^{-1} band intensity decreased significantly within 20.0−44.6 °C, and the 1627.2 cm^{-1} band showed a decrease in intensity within 20.0−35.1 °C. A similar behavior was observed with spectra of GGBP/Glc (data not shown). Within the range of temperature 20.0−59.0 °C the intensity of the main α-helix band (1650.7 cm^{-1}) is almost the same, whereas the intensity of the main *β*-sheet band (1636.6 cm^{-1}) decreases significantly. Concomitantly to the decrease in intensity of the 1658.2, 1627.2, and 1636.6 cm^{-1} bands, an increase in intensity of the 1617.8 cm^{-1} band occurs. The latter phenomenon is due to protein aggregation as a consequence of partial unfolding of above-mentioned secondary structural elements. Indeed, the appearance

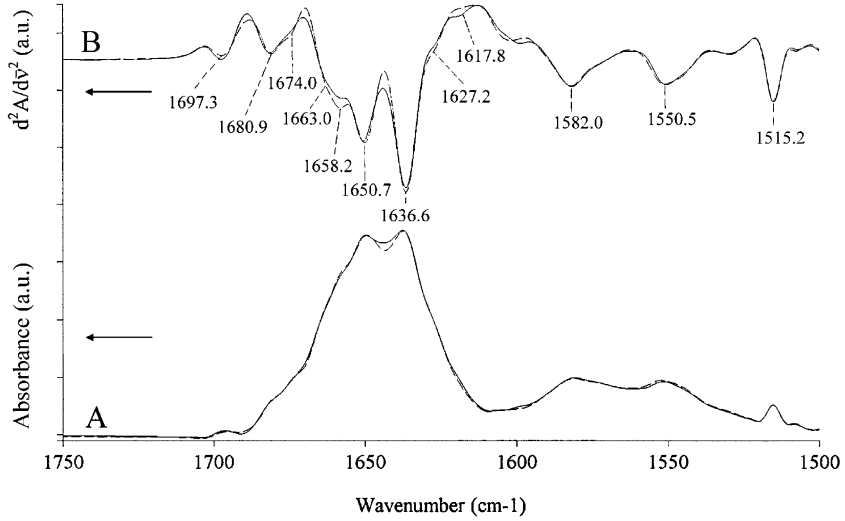

Figure 4. Deconvoluted (A) and second derivative (B) spectra of GGBP and GGBP/Glc in ^2H_2O medium, p^{2}H 7.0 at 20 °C. Continuous and dashed lines refer to spectra of GGBP and GGBP/Glc, respectively.

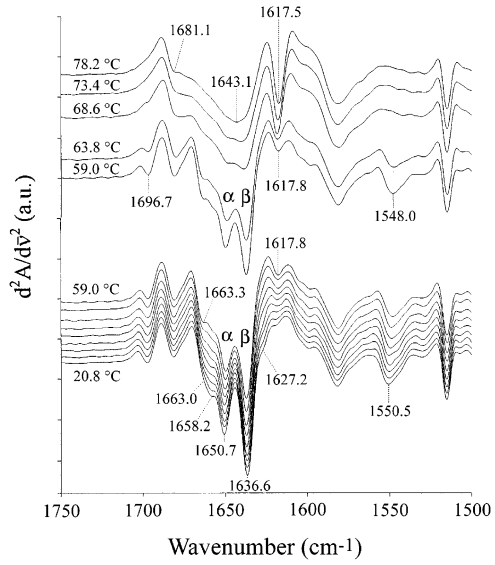

Figure 5. Temperature-dependent changes in the second derivative spectrum of GGBP. The bottom set of spectra comprises spectra recorded at 20.0, 25.5, 30.2, 35.1, 39.9, 44.6, 49.4, 54.2, and 59.0 °C, respectively.

of bands close to 1617 and 1680 cm^{-1} reflects intermolecular interactions (aggregation) brought about by protein denaturation (*25*, *28*−*30*), and they are seen better in the spectra recorded at and above 68.6 °C (Figure 5, upper set of spectra). In these spectra the bands typical of periodical secondary structure elements are very small or absent; at 78.2 °C, a broad band, between the two aggregation peaks and centered at 1643.1 cm^{-1} (unordered structures), characterizes the spectrum. The large loss of secondary structure occurs when the protein sample is heated from 63.8 to 68.6 °C, indicating the temperature of protein melting (T_m) within this range of temperature. Concomitantly to the large protein unfolding, a further and marked $^1H/^2H$ exchange occurs, as indicated by the decrease in intensity of the residual amide II band (1548 cm^{-1}) at 68.6 °C.

Similar temperature-dependent changes were observed with the second derivative and deconvoluted spectra (not shown) of GGBP/Glc, with the difference that T_m and the temperature of further and large $^1H/^2H$ exchange was shifted to higher values. Figure 6 shows the whole scenario. In particular, Figure 6A displays the thermal denaturation curves of GGBP and GGBP/Glc obtained by plotting the amide I′ bandwidth, calculated at one-half of amide I′ band height (W1/2H), as a function of temperature (*30*−*32*). The plot shows that glucose stabilizes the structure of the protein, the T_m of GGBP and of GGBP/Glc being found at 64.5 °C and 70 °C, respectively. As a consequence of protein stabilization induced by glucose, the further and large $^1H/^2H$ exchange in the protein is shifted to higher temperature (Figure 6B). The rate of $^1H/^2H$ exchange depends on the temperature, and it increases when loss of secondary structural elements and/or relaxation of the tertiary structure occur. Hence, the onset of a large $^1H/^2H$ exchange observed at about 60 °C corresponds to the onset of the marked protein unfolding (Figure 6A). Between 20 and 60 °C the $^1H/^2H$ exchange increases to a lower extent, but continuously. This phenomenon may be associated with the fact that the rate of $^1H/^2H$ exchange increases with the increase of temperature, but in our case it may also be due to the decrease in intensity of the 1658.2 and/or 1636.6 cm^{-1} band, i.e., with the partial unfolding of the secondary structures belonging to these bands (Figure 5, bottom set

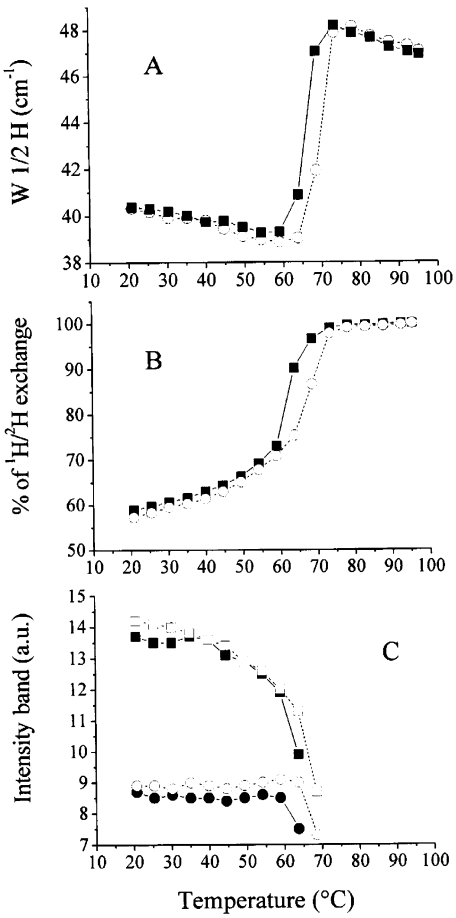

Figure 6. Temperature-dependent changes in amide I′ bandwidth (A), in % of $^1H/^2H$ exchange (B), and in α-helix and β-sheet band intensity (C) for GGBP and GGBP/Glc. Thermal denaturation curves (A) were obtained by monitoring the amide I′ bandwidth, calculated at one-half of amide I′ band height, as a function of the temperature: (■) GGBP; (○) GGBP/Glc. The percentage of $^1H/^2H$ exchange (B) was calculated as reported in Materials and Methods: (■), GGBP; (○) GGBP/Glc. The intensity of the main α-helix (1658.2 cm^{-1}) and β-sheet band (1636.6 cm^{-1}), in the second derivative spectra of proteins (C), were multiplied by a factor of 10^4 and plotted as a function of the temperature. The plot stops at temperatures around 70 °C because of the disappearance of the signal under investigation: (■) β-sheet signal in GGBP spectra; (□) β-sheet signal in GGBP/Glc spectra; (●) α-helix signal in GGBP spectra; (○) α-helix signal in GGBP/Glc spectra. Similar plots were obtained with deconvoluted spectra (not shown).

of spectra). In particular, the decrease in intensity of the main β-sheet band (1636.6 cm^{-1}) fits well with the $^1H/^2H$ exchange data since the second derivative signal decreases continuously and with similar steps till 60 °C and then drops markedly in correspondence of large unfolding (Figure 6C). Conversely, the second derivative signal related to the main α-helix band is almost constant till 60 °C, indicating that α-helices are more stable than β-sheets within the range of temperature 20−60 °C (Figure 6C).

Fluorescence Spectroscopy. In Figure 7 are shown the steady-state emission spectra of GGBP (Figure 7A) and GGBP/Glc (Figure 7B). The tryptophan emission spectra of the protein are similar both in the absence and in the presence of the sugar. The maximum of the fluorescence emission is centered at 344 nm and is blue-shifted compared with the emission maximum of *N*-acetyltryptophanamide (data not shown) (*33*). GGBP possesses five tryptophan residues, and our data show that the addition of glucose at 20 °C does not affect the

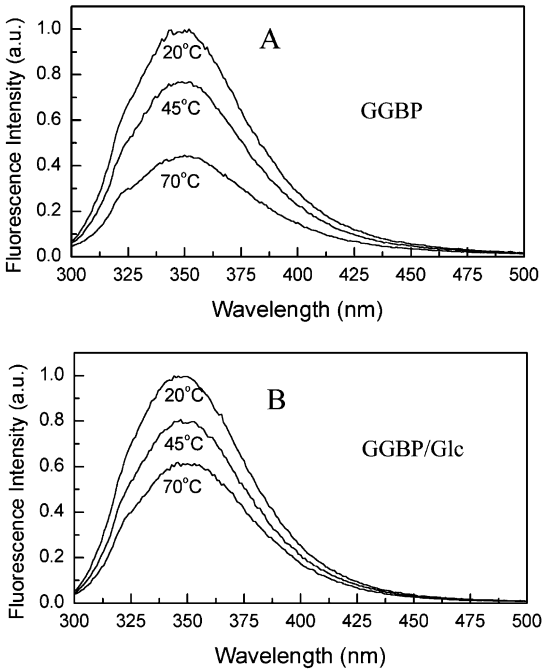

Figure 7. Steady-state emission spectra of GGBP and GGBP/Glc in the range of temperature 20−75 °C.

emission of the indolic residues of the protein. In Figure 7 is also shown the effect of the addition of glucose on the stability of GGBP in the range of temperature 20−70 °C. When the temperature is raised to 70 °C, the fluorescence emission of GGBP and GGBP/Glc linearly decreases. However, the fluorescence emission of GGBP/Glc decreases less than that of GGBP alone, suggesting that, in the range of temperature between 20 and 70 °C, GGBP/Glc is more stable than GGBP.

To estimate the extent of GGBP tryptophan shielding from the solvent we examined the collisional quenching by acrylamide. Acrylamide is a highly water soluble and polar substance that does not penetrate the hydrophobic interior of proteins (*34*, *35*). In Figure 8 is depicted the effect of acrylamide on the fluorescence emission of GGBP and GGBP/Glc at 25 and 45 °C. Addition of acrylamide to the protein solution at 25 °C results in a Stern−Volmer plot moderately curved downward, suggesting that at this temperature some of GGBP indolic residues might be almost completely buried in the protein matrix. The Stern−Volmer plots are the same for GGBP both in the absence and in the presence of glucose, suggesting that at 25 °C the presence of glucose does not affect the protein tryptophan shielding. The calculated Stern−Volmer quenching constants K_{SV} and the bimolecular quenching constants k_q (calculated from the intensity average lifetimes showed in Table 2) are 3.4 M^{-1} and 1.1 × 10^9 M^{-1} s^{-1}, respectively, indicating that the GGBP indolic residues are accessible to the solvent at about 20% of the diffusion controlled rate. At 45 °C, it appears evident that the quencher's accessibility to the tryptophan residues of GGBP is higher in the absence of glucose. At 45 °C the calculated K_{SV} constants for GGBP and GGBP/Glc are the same, which is K_{SV} = 3.5 M^{-1}. The quenching rate constants (k_q) at 45 °C are 2.2 × 10^9 M^{-1} $s^{-1}$and 1.7 × 10^9 M^{-1} s^{-1}, for GGBP and GGBP/Glc, respectively (*33*). These results show that at 45 °C the protein tryptophan residues of GGBP are more accessible to the solvent than the indolic residues of GGBP/Glc, suggesting that the protein in the presence of glucose assumes a more compact structure (*36*−*39*).

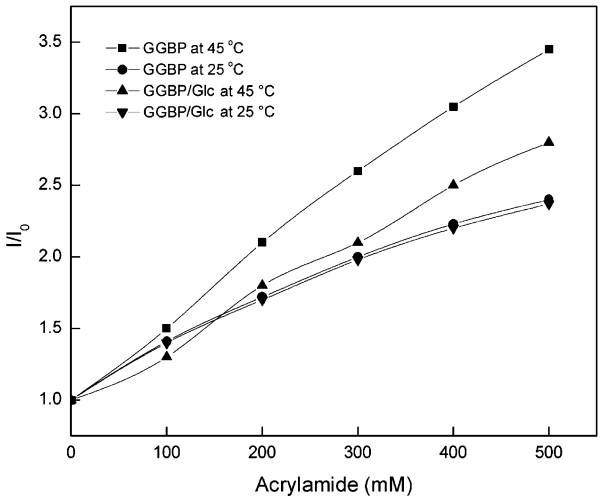

Figure 8. Effect of acrylamide on the fluorescence emission GGBP and GGBP/Glc at different temperatures.The fluorescence data were corrected for the dependence of temperature (*33*). The Stern−Volmer plots were calculated according to Eftink (*43*).

Table 2. Multiexponential Analysis of GGBP and GGBP/Glc at Various Temperatures[a]

temp (°C)	⟨t⟩ (ns)	τ_1 (ns)	τ_2 (ns)	τ_3 (ns)	α_1	α_2	α_3	f_1	f_2	f_3	$\chi 2$
					GGBP						
20	6.08	0.38	3.00	8.53	0.15	0.57	0.27	0.01	0.42	0.56	1.3
45	5.53	0.51	2.70	9.00	0.20	0.62	0.17	0.03	0.50	0.46	1.1
75	5.10	0.36	1.60	8.00	0.20	0.24	0.07	0.07	0.37	0.56	1.4
					GGBP/Glc						
20	6.20	0.33	3.30	8.80	0.15	0.66	0.30	0.01	0.44	0.54	1.1
45	5.78	0.72	2.90	9.50	0.30	1.10	0.30	0.03	0.51	0.45	1.2
75	5.31	0.32	1.70	8.60	0.30	0.63	0.16	0.03	0.43	0.53	1.3

[a] See Material and Methods section for experimental details.

To investigate the conformational dynamics of GGBP and GGBP/Glc the fluorescence intensity decays were measured by using the frequency-domain method (*40*, *41*). The data were analyzed in terms of multiexponential models. In all cases, the best fits were obtained by using the three exponential model, characterized by χ^2 values much lower than those obtained by applying simpler models (data not shown). At 20 °C, GGBP shows three lifetime components at 0.38, 3.00, and 8.53 ns. Increasing the temperature to 45 °C results in a moderate increase of the short-lived and long-lived components from 0.38 and 8.53 ns to 0.51 and 9.0 ns, respectively. The middle-lived component decreases from 3.00 to 2.77 ns. Finally, at 75 °C, we observe a marked decrease of all three protein components (τ_1 = 0.36 ns, τ_2 = 1.63 ns, and τ_3 = 8.00 ns).

At 20 °C, GGBP/Glc displays three lifetime components centered at 0.33, 3.30, and 8.80 ns. Increasing the temperature to 45 °C, we observed a marked increase of the short-lived and long-lived components from 0.33 and 8.80 ns to 0.72 and 9.50 ns, respectively. The middle-lived component decreases from 3.30 to 2.90 ns. At 75 °C, the middle-lived component decreases from 2.90 to 1.74 ns, while the short-lived and long-lived components decrease from 0.72 and 9.50 ns to 0.32 and 8.60 ns, respectively.

The modest increases in the individual components of intensity decays may be a consequence of the multi-exponential model used to fit the experimental data. However, it is worth mentioning that the average lifetime decreases with the increasing temperature.

Discussion

The periplasmic binding protein GGBP can bind several monosaccharides (D-glucose, D-galactose, L-arabinose, L-xylose) with different affinity constants. In fact, GGBP binds glucose with a dissociation constant near 0.8 μM and the other sugars with affinity constants 100- to 1000-fold weaker than that of glucose (*4*). GGBP belongs to a diverse group of proteins including a variety of lysozymes, metabolic enzymes, kinases, nucleic acid binding proteins, and small molecule binding proteins, which trap substrate in a hinged cleft between two domains (*42*). Upon interaction with its saccharide ligands, GGBP undergoes a conformational change to facilitate the interaction of bound GGBP to the membrane-anchored chemoreceptor.

The secondary structure content derived from FT-IR experiments is consistent with that obtained from CD and with that derived from X-ray diffraction (*8*). Moreover, both the FT-IR and CD data indicate that the addition of glucose slightly increases the content of α-helices of GGBP. Besides these small changes in the secondary structure, glucose induces a stabilization of the GGBP molecule against high temperatures. CD data showed that T_m of GGBP and GGBP/Glc is about 58 and 64 °C, respectively. Infrared data also indicate that glucose stabilizes the structure of the protein, but the T_m of GGBP and of GGBP/Glc was found at about 64.5 and 70 °C, respectively. This discrepancy with CD data may be explained by the high concentration of protein used in the infrared experiment (about 40 mg/mL) as compared to the concentration used in the CD measurements (0.2 mg/mL), as well as by the difference in sensitivity of the two techniques for detecting α-helices (*29*, *43*, *44*). The stabilization of the structure, induced by glucose binding, renders the protein slightly less accessible to the solvent at 20−25 °C, as indicated by infrared and fluorescence data. At 20 °C the $^1H/^2H$ exchange calculations revealed about 42% of the GGBP structure not accessible to ^2H_2O, which is a high value for a soluble protein. In the presence of glucose the $^1H/^2H$ exchange was lower, which is consistent with the fact that the glucose-binding site is small as compared to the whole protein structure and that it is located in a solvent-accessible cleft of GGBP (*8*). In this cleft the binding of glucose involves some amino acids in a network of hydrogen bonds, thus protecting the amide hydrogens against the exchange with deuterium. The time-resolved fluorescence data indicate that the glucose binding does not affect the conformational dynamics of GGBP, indicating that the observed protein stabilization induced by the binding of glucose could be overall related to secondary structural elements of GGBP. The presence of secondary structural elements particularly sensitive to temperature has been revealed by infrared spectra. Although they represent a small part of the whole structure, they might be of functional and/or structural importance. It has been shown that glucose increases the content of the α-helix (1658.2 cm^{-1} band), and this increase has been confirmed by CD spectroscopy. Moreover, the thermal denaturation experiments revealed that this particular helix is sensitive to temperature within 20−44 °C, a range that comprises the optimal growth temperature of *E. coli*. Much more sensitive to the temperature is (are) the β-strand(s) belonging to the 1627.2 cm^{-1} band, which decreases in intensity within 20−35 °C. These structural features might be of importance also when planning biotechnological applications of GGBP such as, for instance, glucose sensors. It is important, in fact, that the protein possesses a long lifetime, which could be compromised by the presence of some particularly thermally sensitive protein stretches. On the other hand, the other population of β-strands (1636.6 cm^{-1} band) resulted also to be more sensitive to temperature than the population of α-helices belonging to the 1650.7 cm^{-1} band. A small but continuous decrease in intensity of the 1636.6 cm^{-1} band indicated such a phenomenon that generated also protein aggregation at temperatures close to 59 °C. It is interesting to note that at 45 °C the short-lived and long-lived lifetime components increased significantly both in GGBP and GGBP/Glc with the concomitant decrease of the middle-lived component indicating protein conformational changes consistent with the infrared data.

In conclusion, our data indicate that the binding of glucose affects the secondary structure of GGBP, and the observed glucose-induced thermal stabilization of GGBP can represent the basis for the design of novel biosensors.

Acknowledgment

This project was realized in the frame of CRdC-ATIBB POR UE-Campania Mis 3.16 activities (S.D., M.R). This work was also supported by American Diabetic Association (S.D, J.R.L.), by a Grant from Universita' Politecnica delle Marche (F.T), by the Italian National Research Council (S.D, M.R), by F.I.R.B. grant (S.D, M.R), and by the NIH National Centre for Research Resources, R-R 08119.

References and Notes

(1) Boos, W.; Lucht, J. M. Periplasmic binding-protein-dependent ABC transports. In *E. coli and Salmonella typhimurium: Cellular and Molecular Biology*; Lin, E., Ed.; American Society for Microbiology: Washington, DC, 1995; pp 1175−1209.

(2) Quicho, F. A. Atomic structures and function of periplasmic receptors in active transport and chemotaxis. *Curr. Opin. Biol.* **1991**, *1*, 922−933.

(3) Flocco, M. M.; Mowbray, S. L. The 1.9 Å X-ray structure of a closed unliganded form of the periplasmic glucose\galactose receptor from *Salmonella typhimurium*. *J. Biol. Chem.* **1994**, *269*, 8931−8936.

(4) Tolosa, L.; Gryczynski, I.; Eichhorn, L. R.; Dattelbaum, J. D.; Castellano, F. N.; Rao, G.; Lakowicz, J. R. Glucose sensor for low-cost lifetime-based sensing using a genetically engineered protein. *Anal. Biochem.* **1999**, *267*, 114−120.

(5) Luck, L. A.; Falke, J. J. Open conformation of a substrate binding cleft: ^{19}F NMR studies of cleft angle in the D-galactose chemosensory receptor. *Biochemistry* **1991**, *30*, 6484−6490.

(6) Gilardi, G.; Zhou, L. Q.; Hibbert, L.; Cass, A. E. G. Engineering the maltose binding protein for reagentless fluorescence sensing. *Anal. Chem.* **1994**, *66*, 3840−3847.

(7) Marvin J. S.; Hellinga, H. W. Engineering biosensors by introducing fluorescent allosteric signal transducers: Construction of a novel glucose sensor. *J. Am. Chem Soc.* **1998**, *120*, 7−11.

(8) Vyas, N. K.; Vyas, M. N.; Quiocho, A. Sugar and signal-transducer binding sites of the *Escherichia coli* galactose chemoreceptor protein. *Science* **1988**, *242*, 1290−1295.

(9) Salins, L. L.; Ware, R. A.; Ensor, C. M.; Daunert, S. A novel reagentless sensing system for measuring glucose based on the galactose/glucose-binding protein. *Anal. Biochem.* **2001**, *294*, 19−26.

(10) D'Auria, S.; Lakowicz, R. J. Enzyme fluorescence as a sensing tool: new perspectives in biotechnology. *Curr. Opin. Biotechnol.* **2001**, *12* (1), 99−104.

(11) Bradford, M. M. A rapid and sensitive method for the quantification of microgram quantities of protein utilizing the principle of protein-dye binding. *Anal. Biochem.* **1976**, *72*, 248−254.

(12) D'Auria, S.; Rossi, M.; Barone, G.; Catanzano, F.; Del Vecchio, P.; Graziano, G.; Nucci, R. Temperature-induced denaturation of beta-glycosidase from the archaeon *Sulfolobus solfataricus*. *J. Biochem*. **1996**, *120*, 292−300.

(13) Salomaa, P.; Schaleger, L. L.; Long, F. A. Solvent deuterium isotope effects on acid−base equilibria. *J. Am. Chem. Soc*. **1964**, *86*, 1−7.

(14) Tanfani, F.; Galeazzi, T.; Curatola, G.; Bertoli, E., Ferretti, G. Reduced β-strand content in apoprotein B-100 in smaller and denser low-density lipoprotein subclasses as probed by Fourier transform infrared spectroscopy. *Biochem. J*. **1997**, *322*, 765−769.

(15) Osborne, H. B.; Nabedryk-Viala, E. Infrared measurements of peptide hydrogen exchange in rhodopsin. *Methods Enzymol*. **1982**, *88*, 676−680.

(16) Capasso, C.; Abugo, O.; Tanfani F.; Scirè, A.; Carginale, V.; Scudiero, R.; Parisi, E.; D'Auria, S. Stability and conformational dynamics of metallothioneins from the Antarctic fish *Notothenia coriiceps* and mouse. *Proteins* **2002**, *46*, 259−267.

(17) Banuelos, S.; Arrondo, J. L. R.; Goni, F. M.; Pitaf, G. Surface-core relationships in human low-density lipoprotein as studied by infrared spectroscopy. *J. Biol. Chem*. **1995**, *270*, 9192−9196.

(18) Lakowicz, J. R.; Laczko, G.; Gryczynski, I. A 2 GHz frequency-domain fluorometer. *Rev. Sci. Instrum*. **1986**, *57*, 2499−2504.

(19) Laczko, G.; Gryczynski, I.; Gryczynski, Z.; Wiczk, W.; Malak, H.; Lakowicz, J. R. A 10 GHz frequency domain fluorometer. *Rev. Sci. Instrum*. **1990**, *61*, 92331−9237.

(20) Lakowicz, J. R.; Laczko, G.; Cherek, H.; Gratton, E.; Limkeman, H. Analysis of fluorescence decay kinetics from variable−frequency phase shifts and modulation data. *Biophys. J*. **1984**, *46*, 463−477.

(21) Arrondo, J. L. R.; Muga, A.; Castresana, J.; Goñi, F. M. Quantitative studies of the structure of proteins in solutions by Fourier transform infrared spectroscopy. *Prog. Biophys. Mol. Biol*. **1993**, *59*, 23−56.

(22) Tanfani, F.; Lapathitis, G.; Bertoli, E.; Kotyk, A. Structure of yeast plasma membrane H^+-ATPase: comparison of activated and basal-level enzyme forms and effects of AMP-PNP and diethylstilbestrol. *Biochim. Biophys. Acta* **1998**, *1369*, 109−118.

(23) Surewicz, W. K.; Mantsch, H. H.; Chapman, D. Determination of protein secondary structure by Fourier transform infrared spectroscopy: A critical assessment. *Biochemistry* **1993**, *32*, 389−394.

(24) Casal, H. L.; Kohler, U.; Mantsch, H. H. Structural and conformational changes of β-lactoglobulin B: an infrared spectroscopic study of the effect of pH and temperature. *Biochim. Biophys. Acta* **1988**, *957*, 11−20.

(25) Jackson, M.; Mantsch, H. H. Beware of proteins in DMSO. *Biochim. Biophys. Acta* **1991**, *1078*, 231−235.

(26) Krimm, S.; Bandekar, J. Vibrational spectroscopy and conformation of peptides, polypeptides and proteins. *Adv. Protein Chem*. **1986**, *38*, 181−364.

(27) Chirgadze, Y. N.; Fedorov, O. W.; Trushina, N. P. Estimation of amino acid residue side-chain absorption in the infrared spectra of protein solutions in heavy water. *Biopolymers* **1975**, *14*, 679−694.

(28) Jackson, M.; Mantsch, H. H. Halogenated alcohols as solvents for proteins: FTIR spectroscopic studies. *Biochim. Biophys. Acta* **1992**, *1118*, 139−143.

(29) D'Auria, S.; Barone, R.; Rossi, M.; Nucci, R.; Barone, G.; Fessas, D.; Bertoli, E.; Tanfani, F. Effects of temperature and SDS on the structure of β-glycosidase from the thermophilic archaeon *sulfolobus solfataricus. Biochem. J*. **1997**, *323*, 833−840.

(30) Fernandez-Ballester, G.; Castresana, J.; Arrondo, J. L.; Ferragut, J. A.; Gonzalez-Ros, J. M. Protein stability and interaction of the nicotinic acetylcholine receptor with cholinergic ligands studied by Fourier transform infrared spectroscopy. *Biochem. J*. **1992**, *288*, 421−426.

(31) Tanfani, F.; Scirè, A.; Masullo, M.; Raimo, G.; Bertoli, E.; Boccchini, V. Salts induce structural changes in the elongation factor 1α from the hyperthermophilic archaeon *Sulfolobus solfataricus*: a Fourier transform infrared spectroscopic study. *Biochemistry* **2001**, *40*, 13143−13148.

(32) Muga, A.; Cistola, D. P.; Mantsh, H. H. A comparative study of the conformational properties of *Escherichia coli* derived rat intestinal and liver fatty acid binding proteins. *Biochim. Biophys. Acta* **1993**, *1162*, 291−296.

(33) Lakowicz, J. R. In *Principles of Fluorescence Spectroscopy*; Plenum Press: New York, 1999.

(34) Eftink, M. R. *Topics in Fluorescence Spectroscopy*; Lakowicz, J. R., Ed.; Plenum Press: New York, 1992; Vol. III.

(35) Eftink, M. R.; Ghiron, C. A. Exposure of tryptophanyl residues in Proteins. Quantitative determination by fluorescence quenching studies. *Biochemistry* **1976**, *15* (3), 672−680.

(36) Eftink, M. R.; Ghiron, C. A. Fluorescence quenching of indole and model micelle systems. *J. Phys. Chem*. **1976**, *80* (5), 486−493.

(37) Eftink, M. R.; Selvidge, L. A.; Callis, P. R.; Rehms, A. A. Photophysics of indole derivates: experimental resolution of 1La and 1Lb transitions and comparisons with theory. *J. Phys. Chem*. **1990**, *19*, 125−140.

(38) D'Auria, S.; Nucci, R.; Rossi, M.; Gryczniski, I.; Gryczniski, Z.; Lakowicz, J. R. The β-glycosidase from the hyperthermophilic archaeon *Sulfolobus solfataricus*: enzyme activity and conformational dynamics at temperatures above 100 °C. *Biophys. Chem*. **1990**, *13*, *81* (1), 23−31.

(39) Hong-Tao, M.; Vela, F.; Fronczek, M.; Mc Laughim, M. D. Barkley Micro-environmental effects on the solvent quenching rate in constrained tryptophan derivates. *J. Am. Chem. Soc.* **1995**, *117*, 348−358.

(40) Lakowicz, J. R.; Grycznyski, I. Frequency-domain fluorescence spectroscopy. In *Topics in Fluorescence Spectroscopy, Volume 1: Techniques*; Plenum Press: New York, 1991; pp 293−335.

(41) Lakowicz, J. R.; Lackzo, G.; Cherek, H.; Gratton, E.; Limkeman, H. Analysis of fluorescence decay kinetic from variable frequency phase shifts and modulation data. *Biophys. J*. **1984**, *46*, 463−477.

(42) Careaga, C. L.; Sutherland, J.; Sabeti, J.; Falke, J. J. Large amplitude twisting motions of an interdomain hinge: a disulphide trapping study of the galactose-glucose binding protein. *Biochemistry* **1999**, *34*, 3048−3055.

(43) D'Auria, S.; Rossi, M.; Nucci, R.; Irace, G.; Bismuto, E. Perturbation of conformational dynamics, enzymatic activity, and thermostability of beta-glycosidase from archaeon *Sulfolobus solfataricus* by pH and sodium dodecyl sulfate detergent. *Proteins* **1997**, *27*, 71−79.

(44) D'Auria, S.; Herman, P.; Lakowicz, J. R.; Tanfani, F.; Bertoli, E.; Manco, G.; Rossi, M. The esterase from the thermophilic eubacterium *Bacillus acidocaldarius*: structural-functional relationship and comparison with the esterase from the hyperthermophilic archaeon *Archaeoglobus fulgidus. Proteins* **2000**, *40*, 473−481.

Accepted for publication August 5, 2003.

BP0341848